Incorporation of Nonmetal Impurities at the Anatase $TiO_2(001)$-(1×4) Surface

Jun Hee Lee,[1,*] Daniel Fernandez Hevia,[2] and Annabella Selloni[1]

[1]*Department of Chemistry, Princeton University, Princeton, New Jersey 08544, USA*

[2]*Universidad de Las Palmas de Gran Canaria, Campus de Tafira, 35017 Las Palmas de Gran Canaria, Spain*

(Received 7 September 2012; revised manuscript received 22 October 2012; published 2 January 2013)

We use first principles calculations to investigate the adsorption and incorporation of nonmetal impurities (N, C) at the anatase $TiO_2(001)$-(1×4) reconstructed surface. We analyze in detail the influence of the surface structure and local strain on the impurity binding sites and incorporation pathways and identify important intermediates that facilitate impurity incorporation. We find various subsurface interstitial binding sites and corresponding surface → subsurface penetration pathways on the reconstructed surface. This surface also favors the presence of subsurface oxygen vacancies, to which adsorbed species can migrate to form substitutional impurities. Most notably, we show that the nonexposed oxygen sites just below the surface have a key role in the incorporation of nitrogen and carbon in $TiO_2(001)$.

DOI: 10.1103/PhysRevLett.110.016101 PACS numbers: 68.55.Ln, 68.35.B−, 68.35.Gy, 71.15.Mb

Titanium dioxide (TiO_2) is widely used in photocatalysis [1–4] and solar energy conversion [5–7], yet it is not very efficient. One of the most serious drawbacks of TiO_2 is its large band gap, $E_g \sim 3.2$ eV, which results in the absorption of only a small portion of the solar spectrum in the UV region. An essential prerequisite for increasing the photocatalytic efficiency of TiO_2 is to reduce its band gap. Asahi *et al.* [8] first suggested that this can be achieved using anion dopants, particularly nitrogen, to replace lattice oxygen. The huge amount of experimental and theoretical studies that followed has clarified the electronic structure of anion-doped TiO_2 to a large extent [9–12]. Still, important questions remain, such as those concerning the factors that limit the impurity incorporation in TiO_2 and the influence of doping on the overall photochemical activity [5,13].

The physico-chemical properties of specific surfaces also play a key role in photocatalysis [14,15]. Here we focus on the anatase $TiO_2(001)$ surface that was predicted to be very reactive on the basis of first principles calculations [16,17] and has thus attracted considerable interest in recent years. Since this is usually a minority surface for the anatase form of TiO_2 [14], procedures to grow crystalline anatase samples with a high percentage of (001) facets have been developed, including wet chemical methods with hydrofluoric acid as the crystallographic controlling agent[18] and epitaxial film techniques under vacuum conditions [19]. In this Letter we refer mainly to the latter samples, whose surface properties have been characterized in greater detail. Experimentally, the (001) surface is found to exhibit a (1×4) reconstruction that is stable in a wide temperature range and under a variety of conditions [20,21]. This reconstruction is present also on the surface of N-doped samples [13,19], which is interesting because of two interrelated effects. On the one hand, studies on silicon and other semiconductors have shown that the surface structure and intrinsic stress have an important influence on the incorporation and spatial distribution of impurities [22], suggesting that similar effects may take place also at the $TiO_2(001)$ surface. On the other hand, surface and subsurface impurities are expected to substantially affect the photochemical properties, implying that knowledge of the impurity distribution in the surface region is important for understanding the influence of doping on the photocatalytic activity [23]. Despite the widespread interest in the anatase (001) surface, its capability to accommodate impurities has not yet been explored.

In this Letter we use first principles density functional theory (DFT) calculations to investigate the adsorption and incorporation of nonmetal impurities at the anatase $TiO_2(001)$ surface. We focus on nitrogen, which has attracted much attention in recent years, but, for comparison, we examine also carbon, another widely used p-type dopant [24]. Experimentally, N-doped anatase (001) films can be prepared by codeposition of oxygen and nitrogen during epitaxial growth [19] or by sputtering a preexisting TiO_2 film in an N_2 containing gas [8]. As a simplified model, we consider an N or C atom arriving on a $TiO_2(001)$ surface that is either stoichiometric or has reducing defects (always present in real samples [19]); we do not include steps, which play a prominent role in typical models of epitaxial growth [25] but do not appear to be essential in the growth of TiO_2 [19]. We examine the character and energetics of adsorption vs interstitial and substitutional doping at different sites of the (1×4)-reconstructed surface, comparing to results for the bulk and analyzing the role of the surface structure in the stability of different species. Starting from adsorbed species, we then study likely incorporation pathways for both interstitial and substitutional impurities and identify key intermediates that can lead to facile impurity incorporation in $TiO_2(001)$.

Our study is based on spin-polarized DFT calculations in the generalized gradient approximation (GGA)

of Perdew-Burke-Ernzerhof [26] and the plane-wave-pseudopotential scheme as implemented in the PWSCF code of the QUANTUM ESPRESSO package [27]. Diffusion pathways and barriers were determined using the nudged elastic band (NEB) method [28]. Additional calculation details are given in the Supplemental Material I [29], while comparative results of selected calculations using the DFT + U scheme [30] are reported in the Supplemental Material IV [29]. To describe the reconstructed $TiO_2(001)$-(1×4) surface, we use the "ad molecule" model [31], which agrees well with the available experimental information and is widely accepted. This model is characterized by added TiO_2 rows forming "ridges" that run parallel to the [010] direction and expose fourfold coordinated Ti atoms (Ti_{4c}). In-between ridges, "terraces," expose fivefold coordinated Ti (Ti_{5c}) and twofold coordinated O (O_{2c}) atoms and have the structure of the unreconstructed surface with a lateral compression along [100]. It is mainly the presence of this lateral compression that strongly stabilizes the reconstructed (001) surface by relieving the large intrinsic tensile stress of the unreconstructed surface [31].

Figure 1 shows the formation energies and several geometries of adsorbed and incorporated nitrogen impurities at the $TiO_2(001)$-(1×4) surface. Because of the presence of many inequivalent sites at the reconstructed surface, a variety of species can be identified. In particular, N^a and N^b denote two different adsorption configurations on the terraces, with N-Ti bonds in (010) and (100) planes, respectively; similarly, $N^a{}_R$ ($N^b{}_R$) indicates N^a (N^b)-type adsorption in the ridge (R) region. From Fig. 1, we can see that these adsorbed species have formation energies similar to those of some subsurface interstitials (N_{i1}-N_{i4}), indicating that subsurface interstitial incorporation is competitive with adsorption on the reconstructed surface. We investigated the effect of the surface reconstruction on the structure and stability of the different species by performing calculations for nitrogen at the unreconstructed $TiO_2(001)$ surface. We found that some structures exist only on the reconstructed surface, notably N^a bonded to a single Ti atom (upper left of Fig. 1). In addition, subsurface interstitials are significantly more stable at the reconstructed surface. The influence of the reconstruction is evident in the case of the N_{i4} subsurface interstitial (bottom right of Fig. 1): due to the local compressive strain in the terraces, the nitrogen interstitial pushes the nearest oxygen ($O_{2'}$) outside the surface and takes its original lattice position, effectively becoming an $N_{O2'}$ substitutional impurity capped by a surface oxygen. The resulting N_{i4} species is energetically more stable than a bulk interstitial, $N_{i\,\mathrm{bulk}}$, by more than 1.1 eV.

The reconstructed surface provides also favorable pathways for N adatoms to migrate below the surface as interstitials. For instance, the $N^b{}_R$ adsorption configuration transforms spontaneously to a subsurface split interstitial,

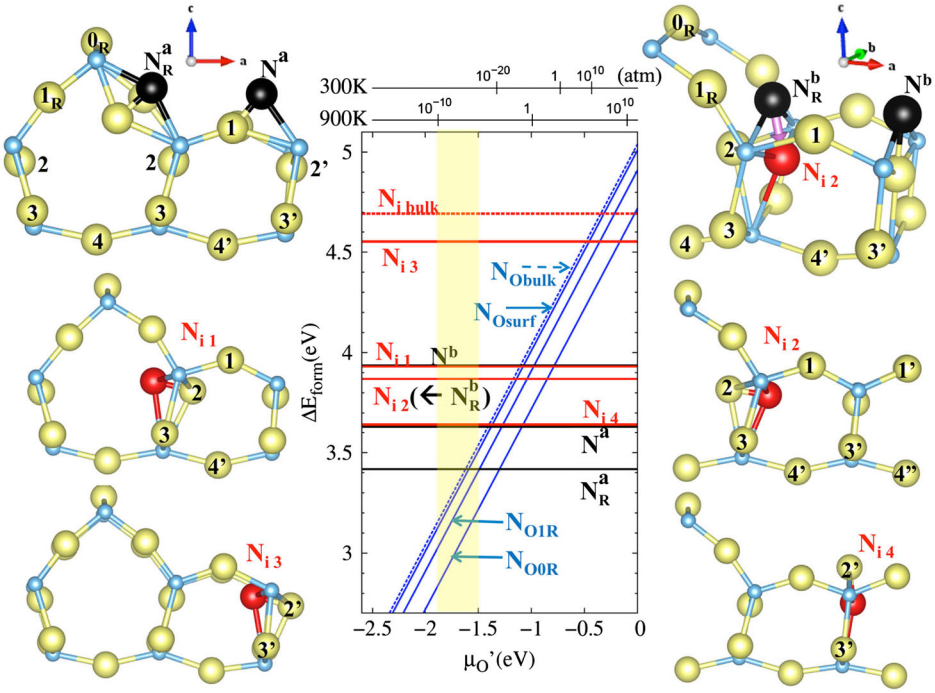

FIG. 1 (color online). Formation energies (eV) vs oxygen chemical potential (μ_O) or O_2 pressure at fixed temperatures ($T = 300$ K and 900 K, top) for N impurities at the anatase $TiO_2(001)$-(1×4) surface. The range of μ_O typically used in experiment is highlighted in yellow. For comparison, the formation energies of substitutional ($N_{O,\mathrm{bulk}}$) and interstitial ($N_{i,\mathrm{bulk}}$) impurities in bulk anatase are also reported. On the left and right sides of the phase diagram inequivalent adsorption and subsurface interstitial structures are shown. Numbers 1–4" indicate inequivalent oxygen sites. Large yellow and small blue spheres represent oxygen and titanium atoms, respectively; adsorbed nitrogen species are black and subsurface nitrogen interstitials are red. The pink arrow in the top right structure indicates the spontaneous relaxation from $N^b{}_R$ to N_{i2}. Directions a, b, c correspond to 100, 010, and 001, respectively. Full slab figures are included in the Supplemental Material II [29].

N_{i2} [top right of Fig. 1 and 2(a)]. The instability of $N^b{}_R$ can be attributed to the fact that the surface reconstruction opens a large space under the ridge around O_2, which can thus move easily to accommodate the adsorbed nitrogen into the interstitial site. Another migration pathway, from N^a to the "substitutional-like" N_{i4} interstitial, is shown in Fig. 2(b). This pathway involves an N^b intermediate, as no direct $N^a \rightarrow N_{i4}$ pathway was found. Interestingly, the energy barrier for the transformation of N^b to N_{i4} is rather low, ~0.6 eV, suggesting that direct adsorption of nitrogen atoms in the N^b configuration would lead to facile incorporation of N impurities. Although N^b adsorption is energetically less stable than N^a (Fig. 1), possibly experimental procedures such as sputtering could increase the population of N^b species, which will subsequently transform to N_{i4} subsurface species. Experimentally a large amount of interstitials has been indeed observed when sputtering has been used to prepare N-doped TiO_2 films [8], whereas a much smaller fraction is present when molecular beam epitaxy is used [13,19]. We also note, however, that while the influence of interstitial impurities on the photocatalytic activity is still unclear [4] and somewhat controversial [12,32], N_{i4} has the structural characteristics of a substitutional impurity rather than an interstitial.

Unlike adsorbed species and interstitials, the formation energies of substitutional impurities depend on the value of the oxygen chemical potential μ_O. Substitutional doping thus becomes the most stable form of nitrogen incorporation for $\mu_O{}' \equiv \mu_O - \frac{1}{2}E_{tot}[O_2] \leq \sim -1.5$ eV, as typically used for the epitaxial growth of anatase TiO_2 [13,20,21] (Fig. 1). At variance with the case of adsorption and interstitial incorporation, the formation energies of substitutional impurities in the terraces ($N_{O\,surf}$) of the reconstructed surface are not significantly different from those in the bulk ($N_{O\,bulk}$), a result consistent with the experimental finding that the maximum concentration of substitutional nitrogen in anatase TiO_2 thin films is ~1% [13], close to that obtained in the bulk [8,33]. However, our calculations also predict that the energetic cost of substitutional doping in the ridge (N_{O0R} and N_{O1R}) is significantly lower compared to that in the bulk, suggesting that the doping concentration in very thin films of anatase TiO_2 might be made higher than in the bulk.

A plausible mechanism for the formation of anionic substitutional impurities is via migration of adatoms to O vacancies (V_O's) below the surface. This mechanism should be quite effective in anatase where subsurface V_O's tend to be more stable than surface V_O's [34,35]. We examined this incorporation pathway for $N^a{}_R$ and N^a adsorbed species migrating to V_{O2} and $V_{O2'}$, respectively (Fig. 3), which are favorable sites for oxygen vacancy formation on the reconstructed (001) surface [34]. We found that the migration barrier is almost vanishing for N^a, on the terrace, whereas it is significant, ~1.0 eV, for $N^a{}_R$ on the ridge. For the latter the migration requires indeed the breaking of a bond with a Ti on the ridge, whereas N^a can smoothly move to the subsurface to form a substitutional $N_{O2'}$ withought breaking any Ti-N bond. It is interesting to remark the close similarity between this $N_{O2'}$ species and the substitutional-like N_{i4}, which, as mentioned earlier, is just $N_{O2'}$ capped by a surface oxygen. Both N_{i4} and $N_{O2'}$ are key intermediates for N

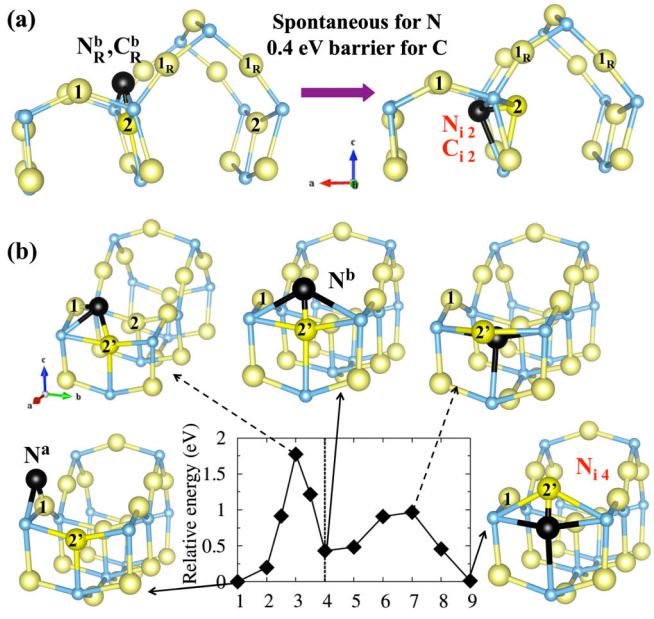

FIG. 2 (color online). Pathways for the incorporation of a N impurity from adsorption to interstitial doping. (a) Spontanous (low-energy barrier) incorporation from $N^b{}_R$ ($C^b{}_R$) to N_{i2} (C_{i2}). (b) Minimum energy pathway (MEP) from N^a to intersitial N_{i4} through an N^b adsorption intermediate. Atomic structures of selected configurations along the MEP are shown. Integers represent the different images in the NEB calculation. Bold (dotted) arrows denote stable (transition) states.

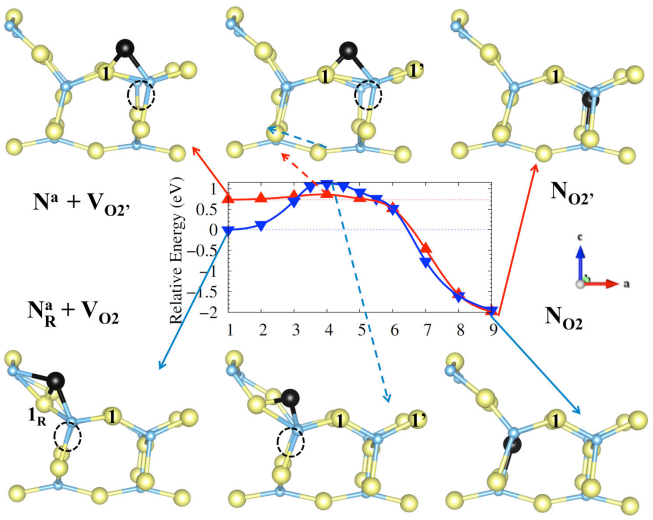

FIG. 3 (color online). MEP for the diffusion of N impurities from the adsorption N^a and $N^a{}_R$ sites to the substitutional $O_{2'}$ (top) and O_2 (bottom) sites, respectively. Atomic structures of selected configurations along the MEP are shown on the bottom. Integers represent the different images in the NEB calculations. Red (blue) dotted arrows denote transition states from N^a ($N^a{}_R$).

incorporation at the $TiO_2(001)$ surface. Their structural similarity suggests that direct interconversion between them can occur, depending on the value of μ_O. As a result, nitrogen incorporation in $TiO_2(001)$ is practically controlled by a single species, $N_{O2'}/N_{i4}$, involving the subsurface $O_{2'}$ sites on the terraces.

Carbon is another frequently used *p-type* dopant in TiO_2 [24]. As shown in Fig. 4(a), for carbon the energetic cost of substitutional incorporation at the $TiO_2(001)$-(1×4) surface is quite high so that, different from nitrogen, substitution is generally unfavorable relative to interstitial doping. However, the most stable C interstitial is C_{i4} [Fig. 4(b)], which is analogous to the N_{i4} species discussed above. Also carbon's incorporation pathways, from adatoms to subsurface interstitials, are similar to those of nitrogen. There is a pathway from $C^b{}_R$ to C_{i2} analogous to the $N^b{}_R \rightarrow N_{i2}$ transformation in Fig. 2(a); the only difference is that, instead of being barrierless as for nitrogen, for carbon there is a barrier of $\sim$0.4 eV (see Supplemental Material V [29]). Analogous to the $N^b \rightarrow N_{i4}$ pathway in Fig. 2(b), there is also a path bringing from adsorbed C^b to the substitutional-like C_{i4}; see Fig. 4(b); although the barrier is quite high, this should still provide a convenient pathway for carbon incorporation at high temperature. Altogether, our calculations indicate that the surface reconstruction affects the adsorption and incorporation of *p*-type dopants nitrogen and carbon in similar ways. In particular, similar to the role of N_{i4} in the case of nitrogen doping, the C_{i4} species is key to carbon incorporation in $TiO_2(001)$.

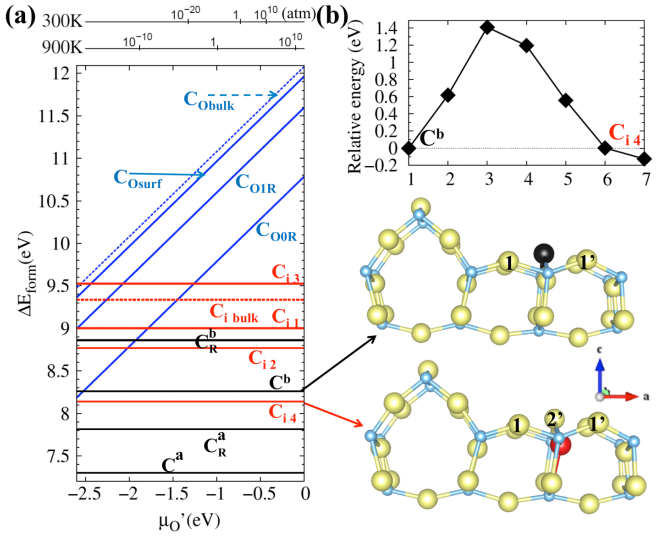

FIG. 4 (color online). (a) Formation energies (eV) vs oxygen chemical potential or O_2 pressure at fixed temperatures (T = 300 K and 900 K, top) for C impurities at the anatase $TiO_2(001)$-(1×4) surface. For comparison, the formation energies of substitutional ($C_{O,bulk}$) and interstitial ($C_{i,bulk}$) impurities in bulk anatase are also reported. Labels of different species are the same as for nitrogen in Fig. 1. Full slab figures are included in the Supplemental Material III [29]. (b) MEP incorporation pathway from adsorption C^b to intersitial C_{i4}. The geometries of these states are also shown.

Once the impurities have been incorporated in the subsurface, they can diffuse toward the bulk. To characterize this process, we assume that diffusion barriers below the second layer are essentially the same as in the bulk. The energy barriers of N and C migration through an oxygen vacancy in the bulk are compared to the oxygen vacancy self-diffusion in Fig. 5. For completeness, also the diffusion of fluorine, an *n*-type nonmetal impurity, is considered. The results show clear trends: the diffusion barriers are large for N and C, they are very small for F, while oxygen is intermediate. These trends can be simply understood considering that N and C tend to form multiple bonds, whereas F prefers to be singly coordinated. Figure 5 shows also a significant anisotropy of the impurity diffusion. Anatase TiO_2 can be considered a layered structure along [001], and the atomic in-plane density is higher than that out of plane. This gives rise to a large anisotropy in Young's modulus and elastic constants, resulting in anatase being stiffer in the xy plane than along the z direction [36]. Moreover, as shown in Fig. 5, an impurity has to break two bonds with Ti atoms in order to migrate along [110] while only one bond needs to be broken for interlayer diffusion along [301]. This explains why out-of-plane diffusion across adjacent TiO_2 layers is significantly more facile than diffusion within the TiO_2 layer for all the investigated impurities. Detailed analyses of the bond length changes and charge states along the impurity diffusion pathways are reported in the Supplemental Material VI [29]. The results show a clear correlation between the computed impurity charge states and diffusion barrier heights.

By combining the results in Figs. 3 and 5, we can see that after an N adatom migrates to the oxygen $O_{2'}$ substitutional site, penetration into the bulk by hopping across adjacent TiO_2 layers has a barrier of 0.63 eV (0.73 eV using DFT + U [37–39]). This is larger than the corresponding oxygen self-diffusion barrier of 0.15 eV (0.39 eV using DFT + U [37–39]), suggesting a poor mobility of N impurities at

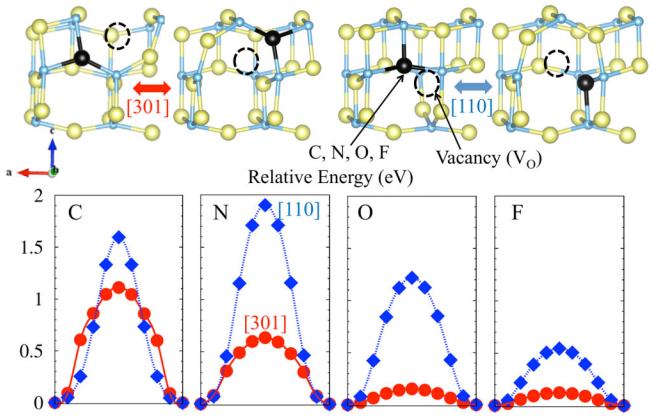

FIG. 5 (color online). Diffusion pathways and corresponding potential energy barriers for C, N, F impurities and for an oxygen vacancy in bulk anatase. Atomic structures of initial and final configurations along the MEP are shown in the upper part of the figure.

room temperature and below. On the other hand, the fact that the oxygen self-diffusion barrier is quite small suggests that electron irradiation of anatase TiO_2 (001) could provide an effective way to create and propagate oxygen vacancies inside the bulk region. This could in turn help N substitutional incorporation into the bulk.

In conclusion, we have presented first principles calculations that provide insights into the mechanisms of incorporation of N and C, two widely used nonmetal impurities, at the reconstructed anatase $TiO_2(001)$-(1×4) surface. Our results point to the central role of surface structure and local stress in determining preferential adsorption and incorporation at selected sites as well as the existence of favorable incorporation pathways and intermediates. In particular, our results show that the subsurface $O_{2'}$ sites in the terraces play a crucial role in the incorporation of nonmetal impurities. The ability to access these sites provides the key to control and/or enhance the incorporation and photochemical activity of anion dopants in $TiO_2(001)$.

We thank Jia Chen for helpful discussions. This research has been supported by Spanish MICINN through Program INNPACTO Project CASCADA IPT-120000-2010-19. We acknowledge the use of computer resources at the TIGRESS high performance computer center of Princeton University, and at the center for Functional Nanomaterials, Brookhaven National Laboratory.

*Corresponding author.
junhee@princeton.edu

[1] A. L. Linsebigler, G. Lu, and J. T. Yates, Chem. Rev. **95**, 735 (1995).
[2] M. R. Hoffmann, S. T. Martin, W. Choi, and D. W. Bahnemann, Chem. Rev. **95**, 69 (1995).
[3] T. L. Thomson and J. T. Yates, Chem. Rev. **106**, 4428 (2006).
[4] M. A. Henderson, Surf. Sci. Rep. **66**, 185 (2011).
[5] M. Grätzel, Nature (London) **414**, 338 (2001).
[6] A. Fujishima, X. Zhang, and D. A. Tryk, Surf. Sci. Rep. **63**, 515 (2008).
[7] X. Chen and S. S. Mao, Chem. Rev. **107**, 2891 (2007).
[8] R. Asahi, T. Morikawa, T. Ohwaki, K. Aoki, and Y. Taga, Science **293**, 269 (2001).
[9] Y. Gai, J. Li, S.-S. Li, J.-B. Xia, and S.-H. Wei, Phys. Rev. Lett. **102**, 036402 (2009).
[10] P. Wang, Z. Liu, F. Lin, G. Zhou, J. Wu, W. Duan, B.-L. Gu, and S. B. Zhang, Phys. Rev. B **82**, 193103 (2010).
[11] C. Di Valentin and G. Pacchioni, Catal. Today (in press).
[12] J. B. Varley, A. Janotti, and C. G. Van de Walle, Adv. Mater. **23**, 2343 (2011).
[13] T. Ohsawa, I. Lyubinetsky, Y. Du, M. A. Henderson, V. Shutthanandan, and S. A. Chambers, Phys. Rev. B **79**, 085401 (2009).
[14] U. Diebold, Surf. Sci. Rep. **48**, 53 (2003).
[15] T. Ohno, K. Sarukawa, and M. Matsumura, New J. Chem. **26**, 1167 (2002).
[16] A. Vittadini, A. Selloni, F. P. Rotzinger, and M. Grätzel, Phys. Rev. Lett. **81**, 2954 (1998).
[17] X. Q. Gong and A. Selloni, J. Phys. Chem. B **109**, 19560 (2005).
[18] H. G. Yang, C. H. Sun, S. Z. Qiao, J. Zou, G. Liu, S. C. Smith, H. M. Cheng, and G. Q. Lu, Nature (London) **453**, 638 (2008).
[19] S. A. Chambers, Adv. Mater. **22**, 219 (2010).
[20] G. S. Herman, M. R. Sievers, and Y. Gao, Phys. Rev. Lett. **84**, 3354 (2000).
[21] Y. Liang, S. Gan, S. A. Chambers, and E. I. Altman, Phys. Rev. B **63**, 235402 (2001).
[22] J. Tersoff, Phys. Rev. Lett. **74**, 5080 (1995).
[23] G. Liu, L. Wang, H. G. Yang, H.-M. Cheng, and G. Q. Lu, J. Mater. Chem. **20**, 831 (2010).
[24] S. Sakthivel and H. Kisch, Angew. Chem., Int. Ed. **42**, 4908 (2003).
[25] J. A. Venables, *Introduction to Surface and Thin Film Processes* (Cambridge University Press, Cambridge, England, 2000).
[26] J. P. Perdew, K. Burke, and M. Ernzerhof, Phys. Rev. Lett. **77**, 3865 (1996).
[27] S. Baroni, P. Giannozzi, S. De Gironcoli, and A. Dal Corso, QUANTUM ESPRESSO, www.democritos.it.
[28] G. Henkelman, B. P. Uberuaga, and H. J. Jonsson, J. Chem. Phys. **113**, 9901 (2000).
[29] See Supplemental Material at http://link.aps.org/supplemental/10.1103/PhysRevLett.110.016101 for details on method, structures, energetics, and charge states.
[30] V. I. Anisimov, J. Zaanen, and O. K. Anderson, Phys. Rev. B **44**, 943 (1991).
[31] M. Lazzeri and A. Selloni, Phys. Rev. Lett. **87**, 266105 (2001).
[32] F. Peng, L. Cai, H. Yu, H. Wang, and J. Yang, J. Solid State Chem. **181**, 130 (2008); F. Peng, Y. Liu, H.-j. Wang, H. Yu, and J. Yang, Chin. J. Chem. Phys. **23**, 437 (2010).
[33] H. Irie, Y. Watanabe, and K. Hashimoto, J. Phys. Chem. B **107**, 5483 (2003).
[34] H. Cheng and A. Selloni, Phys. Rev. B **79**, 092101 (2009).
[35] We notice that formation of subsurface oxygen vacancies is very unfavorable on the unreconstructed $TiO_2(001)$ surface, due to its large tensile strain. Therefore, the substitutional incorporation impurities in the subsurface region is hindered on the unreconstructed surface.
[36] W.-J. Yin, S. Chen, J.-H. Yang, X.-G. Gong, Y. Yan, and S.-H. Wei, Appl. Phys. Lett. **96**, 221901 (2010).
[37] The somewhat higher barrier given by DFT + U relative to the GGA value may be related to the relocation of the vacancy electrons, as found in other recent studies of defect [38] and impurity [39] migration in TiO_2.
[38] P. A. Mulheran, M. Nolan, C. S. Browne, M. Basham, E. Sanvillee, and R. A. Bennett, Phys. Chem. Chem. Phys. **12**, 9763 (2010).
[39] U. Aschauer and A. Selloni, Phys. Chem. Chem. Phys. **14**, 16595 (2012).